



Cite this: DOI: 10.1039/d0cc07292c

 Received 4th November 2020,
Accepted 1st December 2020

DOI: 10.1039/d0cc07292c

rsc.li/chemcomm

Real-time imaging of alkaline phosphatase activity of diabetes in mice *via* a near-infrared fluorescent probe†

 Wen-Xin Wang,^a Wen-Li Jiang,^a Hong Guo,^a Yongfei Li^{ib} ^{ab} and Chun-Yan Li^{ib} ^{*a}

A novel water-soluble near-infrared fluorescent probe named QX-P with simple synthesis is developed. QX-P has high sensitivity and selectivity to ALP. Moreover, the probe can not only visualize ALP activity in four cell lines, but also real-time image ALP activity during the diagnosis and treatment of diabetes in mice.

Diabetes is a kind of metabolic disease characterized by chronic hyperglycemia, which is caused by insulin secretion disorders. It shows many typical symptoms such as polyuria, polydipsia, polyphagia, weight loss and fatigue. If the condition is not treated in time, various tissues and organs will be damaged, especially the kidneys, heart, blood vessels and nervous system.¹ Thus, the prevention and diagnosis of diabetes are essential for the treatment of the disease. Studies have shown that an increase in the alkaline phosphatase (ALP) level may be involved in the pathological process of diabetes.² ALP is a hydrolase that can promote the dephosphorylation of a variety of molecules, and is widely distributed in the liver, kidneys, bones and placenta of mammals.³ ALP activity is generally considered as an important biomarker in clinical diagnosis.⁴ A large amount of evidence shows that abnormally elevated ALP level is closely related to the occurrence of many diseases including breast cancer, prostate cancer, osteoporosis, hepatic disease, and especially, diabetes.⁵ Therefore, it is urgent to develop an analytical means for real-time monitoring of ALP activity during the diagnosis and treatment of diabetes.

So far, many analytical methods for the assay of ALP activity have been reported, such as chromatography, surface enhanced Raman scattering, colorimetric methods and electrochemistry.⁶

Although these provide effective methods for ALP detection, they usually require expensive equipment and complicated operation, and thus are unsuitable for application in organisms. Fluorescent probes have attracted widespread attention due to their prominent characteristics such as low cost, high spatial resolution, high sensitivity and good biocompatibility.⁷ To date, several fluorescent probes have been developed to detect ALP activity,⁸ including tetraphenylethylene, naphthalimide, rhodamine B, coumarin and xanthene. However, their application in biological systems is hindered due to the short emission wavelength (<650 nm) of these probes. Based on the above discussion, the development of suitable fluorescent probes to monitor ALP activity *in vivo* still has great prospects.

In recent years, near-infrared (NIR) fluorescent probes have been vigorously developed and researched due to their deep tissue penetration, little light-damage and low auto-fluorescence interference.⁹ Some hemicyanine-based NIR fluorescent probes have been reported for biological imaging of endogenous ALP.¹⁰ Despite the great efforts, three aspects still need improvement. Firstly, the synthetic routes of these reported probes are complex and depend on the degradation of expensive cyanine dyes (Fig. 1A).^{10a} Secondly, although the emission wavelengths of these reported probes are located in the NIR region, they are basically around 700 nm.^{10a-d} Generally speaking, the longer the emission wavelength, the deeper the penetration depth and the smaller the auto-fluorescence interference. Thirdly, some probes have poor water solubility, which limits their biological application to a certain extent.^{10d,e} Therefore, developing a water-soluble NIR fluorescent probe with long emission wavelength is of great significance for the imaging of ALP activity *in vivo*.

Herein, quinolinium, having a larger conjugated structure and good water solubility, is used to replace indole in the hemicyanine to obtain the fluorophore QX, which shows longer absorption and emission wavelength than the classical hemicyanine dye. The fluorophore is synthesized by cheap raw materials (Fig. 1B). Then, the water-soluble NIR fluorescent probe called QX-P is synthesized, which links a phosphate on the hydroxyl group of QX-OH (Fig. 1C). QX-P itself is non-fluorescent because the intramolecular

^a Key Laboratory for Green Organic Synthesis and Application of Hunan Province, Key Laboratory of Environmentally Friendly Chemistry and Applications of Ministry of Education, College of Chemistry, Xiangtan University, Xiangtan, 411105, P. R. China. E-mail: lichunyan79@sina.com

^b College of Chemical Engineering, Xiangtan University, Xiangtan, 411105, P. R. China

† Electronic supplementary information (ESI) available: Experimental section, synthesis of probes, additional spectral data, response mechanism and supplemental biological assay. See DOI: 10.1039/d0cc07292c

Communication

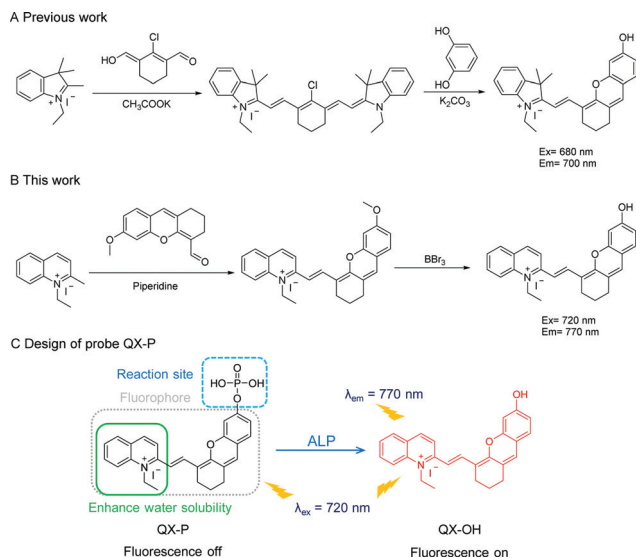


Fig. 1 (A) Previous works: the synthesis of hemicyanine dyes. (B) This work: the synthesis of quinolone-xanthene dyes. (C) Design of probe QX-P to ALP.

charge transfer (ICT) effect is blocked by the phosphate group. After reacting with ALP, the phosphate moiety of QX-P is hydrolyzed and the hydroxyl group is released, causing the ICT process to resume and a strong fluorescent signal at 770 nm appears. QX-P shows excellent selectivity and sensitivity to ALP *in vitro*, and thus is applied for visualizing the activity of ALP in different cells. Furthermore, based on its water solubility and NIR emission characteristic, QX-P has been successfully applied to real-time detection of ALP activity in a diabetic mice model. To our knowledge, QX-P is the first reported fluorescent probe to monitor ALP activity in the diagnosis and treatment of diabetes *in vivo*.

QX-P was synthesized following the synthetic route displayed in Scheme S1 (ESI[†]). The detailed synthetic steps and characterization are given in the ESI[†] (Fig. S1–S6). Firstly, the absorption profiles of QX-P in the absence and presence of ALP were investigated in Tris-HCl buffer solution. As shown in Fig. 2A, the absorption band of QX-P is at 568 nm. After the addition of ALP, the peak at 568 nm significantly decreases and a new absorption band appears at 720 nm accompanied by a color variance from purple to blue. Furthermore, the fluorescence titration experiments between QX-P and ALP were studied. As shown in Fig. 2B, probe QX-P displays a very weak emission at 770 nm. When ALP is added, obvious fluorescence enhancement at 770 nm is observed. With the increase of ALP activity from 0.0 to 1.0 U mL⁻¹, the fluorescence intensity of QX-P enhances around 7-fold. As shown in Fig. 2C, it was found that the fluorescent intensity has a linear relationship with ALP activity in the range 0.05–1.0 U mL⁻¹. And through calculation (ESI[†]), the detection limit (LOD = 3 δ /k) for ALP is 0.017 U mL⁻¹. The above experimental results indicate that QX-P can quantitatively detect ALP activity with high sensitivity.

The effect of pH on the fluorescence of QX-P was investigated as pH is a crucial factor in the enzymatic reaction. As shown in Fig. S7 (ESI[†]), the pH of maximum fluorescence response for ALP is about pH 8.0. Therefore, we chose Tris-HCl buffer

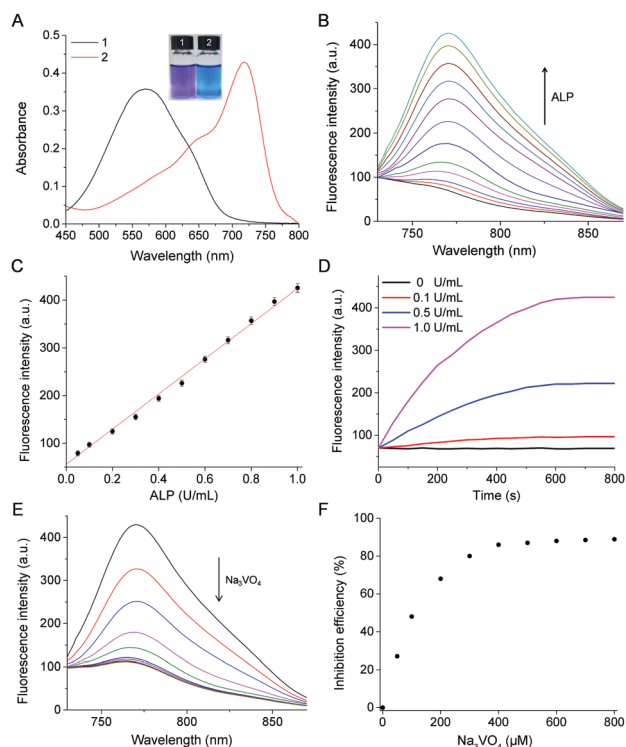


Fig. 2 (A) Absorption spectra of QX-P (10 μM) in the absence (1) and presence (2) of ALP (1.0 U mL⁻¹). Inset: The corresponding color image. (B) Fluorescence spectra of QX-P (10 μM) in the presence of various activities of ALP (0, 0.05, 0.1, 0.2, 0.3, 0.4, 0.5, 0.6, 0.7, 0.8, 0.9, 1.0 U mL⁻¹). (C) Linearity plots of the fluorescence intensity of QX-P versus various activities of ALP. (D) Time-dependent fluorescence response of QX-P (10 μM) upon the addition of ALP (0, 0.1, 0.5, 1.0 U mL⁻¹). (E) Fluorescence spectra of QX-P (10 μM) in the presence of ALP (1.0 U mL⁻¹) at different Na₃VO₄ concentrations (0, 50, 100, 200, 300, 400, 500, 600, 700, 800 μM). (F) The inhibition efficiency versus Na₃VO₄ concentration. All spectra were measured in Tris-HCl buffer solution (50 mM, pH 8.0) at 37 °C. $\lambda_{ex} = 720 \text{ nm}$.

solution with pH 8.0 for subsequent testing. Then, the influence of experimental temperature on the fluorescence response of QX-P before and after the reaction with ALP was measured (Fig. S8, ESI[†]). The results show that the fluorescence intensity reaches the maximum at 37 °C. Hence, 37 °C is chosen as the optimum temperature for the reaction.

The incubation time is another key factor in enzymatic reaction. The time-dependent fluorescence intensity of QX-P with various ALP activities was tested. As shown in Fig. 2D, the fluorescence intensity of QX-P gradually increases with time and reaches the maximum after 10 min. Therefore, an incubation time of 10 min for ALP testing is accepted. Moreover, to optimize the final concentration of QX-P used in the experiment, probes of various concentrations were incubated with unchanging ALP activity. The enzyme kinetics experiment was described by the Michaelis-Menten equation and the result is displayed in Fig. S9A (ESI[†]). The kinetic parameters were calculated by converting the curve to a linear plot by Lineweaver-Burke analysis (Fig. S9B, ESI[†]). According to the slope and intercept of the fitted line, the maximum velocity (V_{max}) and Michaelis constant (K_m) were 0.491 $\mu\text{M min}^{-1}$ and 8.90 μM .

As we all know, the substrate concentration must be higher than its K_m value. Therefore, 10 μM is selected as the optimum QX-P concentration for the ALP assay.

The selectivity of the probe to ALP was studied. From Fig. S10 (ESI[†]), the potential analytes are tested, such as 100 μM metal ions (Na^+ , Ca^{2+} , Mg^{2+}), anions (Cl^- , Br^- , OH^-), reactive oxygen species (ClO^- , O_2^- , H_2O_2), biothiols (GSH, Hcy, Cys), amino acids (Tyr, Pro, Phe, Leu), and 1.0 U mL^{-1} enzymes (acetylcholinesterase, AChE; γ -glutamyl transpeptidase, GGT; phosphodiesterase, PDE; acid phosphatase, ACP). Only ALP can display obvious change of fluorescence intensity, while the other analytes cannot change the fluorescence signal of the probe. This may be owing to the fact that only ALP can catalyze the dephosphorylation process of the probe, and thus a strong fluorescent signal is released. The results indicate that QX-P possesses high selectivity to ALP.

The probe (QX-P) could be used for the screening of ALP inhibitors. To prove this probability, sodium orthovanadate (Na_3VO_4) was studied (Fig. 2E). The fluorescence intensity declines significantly with the increase of Na_3VO_4 concentration. For comparison, the influence of Na_3VO_4 on the fluorescence intensity of QX-OH was also tested, and negligible changes in fluorescence were observed (Fig. S11, ESI[†]). The above results indicate that Na_3VO_4 can effectively inhibit ALP activity. As shown in Fig. 2F, the IC_{50} value (the concentration of an inhibitor reaching 50% of inhibition efficiency) of Na_3VO_4 was estimated to be 109.6 μM . The results strongly suggest that our method can be used to monitor ALP and screen the potential inhibitors of ALP. Moreover, a possible response mechanism of QX-P to ALP was proposed in Scheme S2 (ESI[†]) and proved by the MS, HPLC and DFT calculation (Fig. S12–S14, ESI[†]).

Next, the cytotoxicity of QX-P was investigated in HeLa, HepG2, HCT116 and 4T1 cells by MTT assay (Fig. S15, ESI[†]). More than 90% cell viability is found after the cells are incubated for 24 h with different concentrations of QX-P from 0 to 30 μM , which indicates that the probe has low cytotoxicity in the cells. As we all know, ALP is overexpressed in HeLa, HepG2, HCT116 and 4T1 cells.¹¹ Thus, the four types of cells were used as models for intracellular imaging of ALP activity. As shown in Fig. 3A and Fig. S16 (ESI[†]), the four types of cells untreated with QX-P show hardly any fluorescence signal, which shows that the possibility of auto-fluorescence interference is ruled out. After the cells are incubated with QX-P, a significant red fluorescence is observed, which is caused by the presence of ALP in the four cells. Meanwhile, the fluorescence signal gradually enhances with time and reaches the maximum at 30 min, which shows that QX-P has good cell permeability and can react with ALP in the cells (Fig. S17, ESI[†]). In order to prove the fact that the fluorescence signal was activated by the endogenous ALP in the four cells, the cells were pretreated with Na_3VO_4 (ALP inhibitor) and then treated with QX-P. As expected, a negligible fluorescence signal in the cells was observed. The above results indicate that the enhancement of fluorescence signal in the four cells indeed resulted from endogenous ALP. To more intuitively reflect the changes in the intracellular fluorescence, 3D imaging on each cell

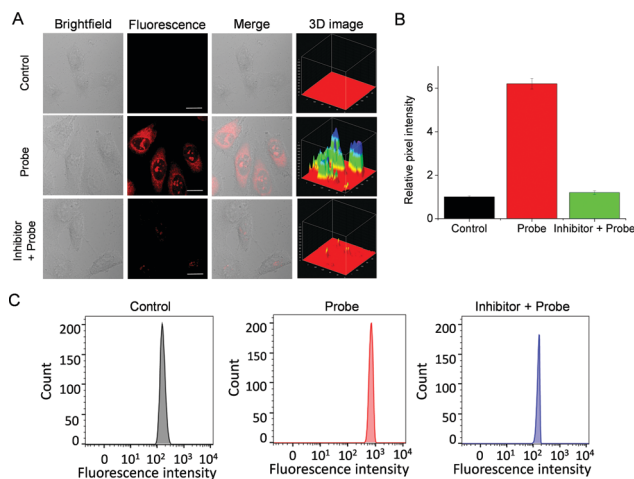


Fig. 3 (A) Fluorescence images of HeLa cells. Control group: the cells were untreated with QX-P; probe group: the cells were treated with QX-P only; inhibitor + probe group: the cells were treated with Na_3VO_4 and QX-P. (B) Relative pixel intensity in (A). (C) Flow cytometry analysis. $\lambda_{\text{ex}} = 640 \text{ nm}$, $\lambda_{\text{em}} = 700\text{--}775 \text{ nm}$. Scale bar: 10 μm .

was performed. Meanwhile, flow cytometry analysis was performed (Fig. 3C and Fig. S18, ESI[†]) and the results were consistent with the above confocal microscopy images. The above experimental phenomenon indicates that QX-P can well monitor the activity of ALP in cancer cells.

Motivated by the excellent performance of living cells, the ability of probe QX-P for the fluorescence imaging of ALP activity *in vivo* was investigated. As shown in Fig. 4A and B, the fluorescence intensity of normal group mice slowly increases with time, which indicates that QX-P can visualize ALP activity in normal mice. The diabetic mice are obtained by intraperitoneally injecting streptozotocin, an analog of *N*-acetylglucosamine, which is a specific toxin for the pancreatic beta cells.¹² At the same incubation time, the fluorescence signal of the diabetic mice group is significantly stronger than that of the normal group, indicating that ALP activity in diabetic mice is significantly upregulated. Then, the diabetic mice were treated with metformin, which is a biguanide derivative used as an oral hypoglycaemic drug in diabetics, and has a protective effect on the organ of streptozotocin-diabetic mice.¹³ It is observed that the fluorescence signal in the mice reduces significantly after the treatment, indicating the down-regulation of ALP in the treatment group due to the remission of symptoms by the drug.

Subsequently, the mice were dissected and the main organs were acquired. As shown in Fig. 4C, the liver and kidneys of the diabetic mice present relatively stronger fluorescence than the other organs, whereas the liver and kidneys of the normal mice exhibit weak fluorescence. Additionally, the liver and kidneys of the treatment group mice display weaker fluorescence signal compared with diabetic mice. This is because the liver and kidneys are the major metabolic organs and a large amount of ALP accumulates in those two organs under diabetic conditions. Inspired by this fact, QX-P was used to study the ALP activity in mouse blood through fluorescence imaging (Fig. 4D).

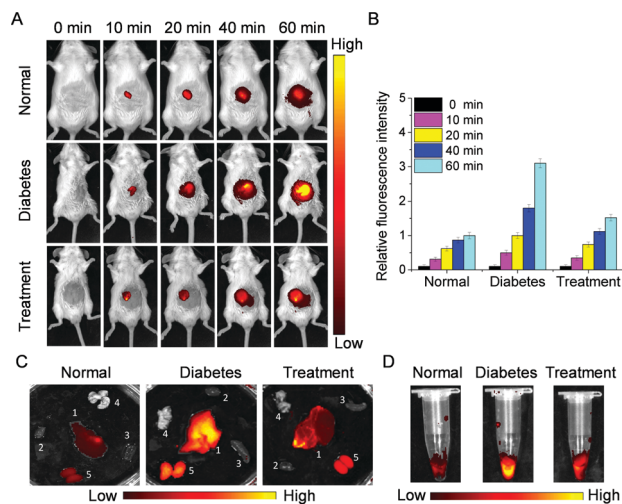


Fig. 4 (A) Fluorescence images of mice from the normal group, diabetes group, and treatment group after injection of QX-P (200 μ M) with time (0, 10, 20, 40, 60 min). (B) Relative fluorescence intensity in (A). The fluorescence intensity of the normal group at 60 min is defined as 1.0. (C) Fluorescence images of major organs. 1: liver, 2: heart, 3: spleen, 4: lungs, 5: kidneys. (D) Fluorescence images of blood from the mice. $\lambda_{\text{ex}} = 640 \text{ nm}$, $\lambda_{\text{em}} = 680\text{--}780 \text{ nm}$.

An obvious fluorescence signal is seen in the diabetes group compared to the normal group, and a significantly weakened fluorescent signal is observed in the treatment group, which is consistent with the above experimental phenomenon. This result indicates that QX-P can be used to monitor the activity of ALP in the diagnosis and treatment of the diabetic mice.

In conclusion, we have, for the first time, reported a water-soluble NIR fluorescent probe (QX-P) based on quinolinium-xanthene dye for detecting ALP activity. Compared with classic hemicyanine dye, the fluorophore QX not only has longer absorption and emission wavelengths, but also has simple synthesis steps and cheap raw materials. QX-P displays excellent sensitivity and selectivity to ALP. Owing to the low cytotoxicity, the probe QX-P can visualize the activity of ALP in different cell lines with outstanding performance. Furthermore, QX-P is used to prove that the ALP level of the diabetic mice is higher than that of normal mice. After treatment with a hypoglycemic drug (metformin), the production of ALP in the diabetic mice is significantly reduced. These results indicate that QX-P could serve as a powerful tool for further studying the clinical value of ALP in the diagnosis and treatment of diabetes.

This work was supported by the National Natural Science Foundation of China (21775133), Hunan Provincial Natural Science Foundation (2018JJ2385), Scientific Research Fund of Hunan Provincial Education Department (19A479), Degree & Postgraduate Education Reform Project of Hunan Province (2019JGYB113) and Degree & Postgraduate Education Reform Project of Hunan Province (CX20190483, XDCX2020B115).

Conflicts of interest

There are no conflicts to declare.

Notes and references

- 1 P. Dayhaw, *Optom. Vis. Sci.*, 1995, **72**, 417–424.
- 2 (a) B. Chua and E. Shrago, *J. Nutr.*, 1978, **108**, 196–202; (b) J. Stěpán, T. Havránek, J. Formánková, J. Skrha, F. Skrha and V. Pacovský, *Clin. Chim. Acta*, 1980, **105**, 75–81.
- 3 (a) J. E. Coleman, *Annu. Rev. Biophys. Biomol. Struct.*, 1992, **21**, 441–483; (b) J. L. Millan, *Purinergic Signalling*, 2006, **2**, 335–341.
- 4 (a) P. H. Lange, J. L. Millan, T. Stigbrand, R. L. Vessella, E. Ruoslahti and W. H. Fishman, *Cancer Res.*, 1982, **42**, 3244–3247; (b) J. B. Warshaw, J. W. Littlefield, W. H. Fishman, N. R. Inglis and L. L. Stolbach, *J. Clin. Invest.*, 1971, **50**, 2137–2142; (c) J. Stebbing, L. C. Lit, H. Zhang, R. S. Darrington, O. Melaiu, B. Rudraraju and G. Giamas, *Oncogene*, 2014, **33**, 939–953.
- 5 (a) H. G. Wada, J. E. Shindelman, A. E. Ortmeier and H. H. Sussman, *Int. J. Cancer*, 1979, **23**, 781–787; (b) J. D. Schmidt, N. H. Slack, T. M. Chu and G. P. Murphy, *J. Urol.*, 1982, **127**, 457–459; (c) P. A. Kyd, K. D. Vooght, F. Kerkhoff, E. Thomas and A. Fairney, *Ann. Clin. Biochem.*, 1998, **35**, 717–725; (d) U. Domar, A. Danielsson, K. Hirano and T. Stigbrand, *Scand. J. Gastroenterol.*, 1988, **23**, 793–800; (e) D. B. Maxwell, E. A. Fisher, H. A. Ross-Clunis and H. L. Estep, *J. Am. Coll. Nutr.*, 1986, **5**, 55–59.
- 6 (a) T. Hasegawa, M. Sugita, K. Takatani, H. Matsuura, T. Umemura and H. Haraguchi, *Bull. Chem. Soc. Jpn.*, 2006, **79**, 1211–1214; (b) C. Ruan, W. Wang and B. Gu, *Anal. Chem.*, 2006, **78**, 3379–3384; (c) C. M. Li, S. J. Zhen, J. Wang, Y. F. Li and C. Z. Huang, *Biosens. Bioelectron.*, 2013, **43**, 366–371; (d) K. Ino, Y. Kanno, T. Arai, K. Y. Inoue, Y. Takahashi, H. Shiku and T. Matsue, *Anal. Chem.*, 2012, **84**, 7593–7598.
- 7 (a) H. W. Liu, L. L. Chen, C. Y. Xu, Z. Li, H. Y. Zhang, X. B. Zhang and W. H. Tan, *Chem. Soc. Rev.*, 2018, **47**, 7140–7180; (b) J. N. Liu, W. B. Bu and J. L. Shi, *Chem. Rev.*, 2017, **117**, 6160–6224; (c) H. Singh, K. Tiwari, R. Tiwari, S. K. Pramanik and A. Das, *Chem. Rev.*, 2019, **119**, 11718–11760; (d) X. F. Wu, W. Shi, X. H. Li and H. M. Ma, *Acc. Chem. Res.*, 2019, **52**, 1892–1904; (e) Y. H. Tang, Y. Y. Ma, J. L. Yin and W. Y. Lin, *Chem. Soc. Rev.*, 2019, **48**, 4036–4048.
- 8 (a) J. Liang, R. T. K. Kwok, H. Shi, B. Z. Tang and B. Liu, *ACS Appl. Mater. Interfaces*, 2013, **5**, 8784–8789; (b) X. F. Hou, Q. X. Yu, F. Zeng, J. H. Ye and S. Z. Wu, *J. Mater. Chem. B*, 2015, **3**, 1042–1048; (c) L. Dong, Q. Miao, Z. Hai, Y. Yuan and G. Liang, *Anal. Chem.*, 2015, **87**, 6475–6478; (d) T. Kim, H. J. Kim, Y. Choi and Y. Kim, *Chem. Commun.*, 2011, **47**, 9825–9827; (e) H. M. Zhang, C. L. Xu, J. Liu, X. H. Li, L. Guo and X. M. Li, *Chem. Commun.*, 2015, **51**, 7031–7034; (f) F. Ma, M. Liu and C. Y. Zhang, *Chem. Commun.*, 2019, **55**, 8963–8966.
- 9 (a) J. Huang, Y. L. Wu, F. Zeng and S. Z. Wu, *Theranostics*, 2019, **9**, 7313; (b) W. Fu, C. X. Yan, Z. Q. Guo, J. J. Zhang, H. Y. Zhang, H. Tian and W. H. Zhu, *J. Am. Chem. Soc.*, 2019, **141**, 3171–3177; (c) M. Gao, R. Wang, F. B. Yu and L. X. Chen, *Biomaterials*, 2018, **160**, 1–14; (d) S. Y. Gong, E. B. Zhou, J. X. Hong and G. Q. Feng, *Anal. Chem.*, 2019, **91**, 13136–13142; (e) Z. Q. Guo, S. Park, J. Yoon and I. Shin, *Chem. Soc. Rev.*, 2014, **43**, 16–29.
- 10 (a) Y. Tan, L. Zhang, K. H. Man, R. Peltier, G. C. Chen, H. T. Zhang, L. Y. Zhou, F. Wang, D. Ho, S. Q. Yao, Y. Hu and H. Y. Sun, *ACS Appl. Mater. Interfaces*, 2017, **9**, 6796–6803; (b) C. S. Park, T. H. Ha, M. Kim, N. Raja, H. S. Yun, M. J. Sung, O. S. Kwon, H. Yoon and C. S. Lee, *Biosens. Bioelectron.*, 2018, **105**, 151–158; (c) Y. Y. Li, H. Song, C. H. Xue, Z. J. Fang, L. Q. Xiong and H. X. Xie, *Chem. Sci.*, 2020, **11**, 5889–5894; (d) H. W. Liu, X. X. Hu, L. M. Zhu, K. Li, Q. M. Rong, L. Yuan, X. B. Zhang and W. H. Tan, *Talanta*, 2017, **175**, 421–426; (e) L. B. Xu, X. He, Y. B. Huang, P. Y. Ma, Y. X. Jiang, X. Liu, S. Tao, Y. Sun, D. Q. Song and X. H. Wang, *J. Mater. Chem. B*, 2019, **7**, 1284–1291; (f) X. T. Gao, G. C. Ma, C. Jiang, L. L. Zeng, S. S. Jiang, P. Huang and J. Lin., *Anal. Chem.*, 2019, **91**, 7112–7117; (g) S. J. Li, C. Y. Li, Y. F. Li, J. J. Fei, P. Wu, B. Yang, J. Ou-Yang and S. X. Nie, *Anal. Chem.*, 2017, **89**, 6854–6860.
- 11 (a) D. Di Lorenzo, A. Albertini and D. Zava, *Cancer Res.*, 1991, **51**, 4470–4475; (b) F. Herz, *Experientia*, 1985, **41**, 1357–1361; (c) H. Matsumoto, R. H. Erickson, J. R. Gum, M. Yoshioka, E. Gum and Y. S. Kim, *Gastroenterology*, 1990, **98**, 1199–1207.
- 12 V. Burkart, Z. Q. Wang, J. Radons, B. Heller, Z. Herceg, L. Stingl, E. F. Wagner and H. Kolb, *Nat. Med.*, 1999, **5**, 314–319.
- 13 D. Stepensky, M. Friedman and I. Raz, *Drug Metab. Dispos.*, 2002, **30**, 861–868.